Ong, Lin Kooi, Zhao, Zidan, Kluge, Murielle, TeBay, Clifford, Zalewska, Katarzyna, Dickson, Phillip W., Johnson, Sarah J., Nilsson, Michael & Walker, Frederick R. "Reconsidering the role of glial cells in chronic stress-induced dopaminergic neurons loss within the substantia nigra? Friend or foe?" Published in *Brain, Behavior, and Immunity*, Vol. 60, February, p. 117-125, (2017).

Available from: http://dx.doi.org/10.1016/j.bbi.2016.10.001

Title page

Journal

Brain, behaviour, and immunity

Title

Reconsidering the role of glial cells in chronic stress-induced dopaminergic neurons loss within the substantia nigra? Friend or foe?

Author names and affiliations

Lin Kooi Ong[1, 2, 3]

Zidan Zhao[1, 2]

Murielle Kluge[1, 2]

Clifford TeBay[1]

Katarzyna Zalewska[1, 2]

Phillip W. Dickson[2, 4]

Sarah J. Johnson[5]

Michael Nilsson [1, 2, 3]

Frederick R. Walker[1, 2, 3]

[1] School of Biomedical Sciences and Pharmacy and the Priority Research Centre for Stroke and Brain Injury, University of Newcastle, Callaghan, NSW, Australia.

[2] Hunter Medical Research Institute, Newcastle, NSW, Australia.

[3] NHMRC Centre of Research Excellence Stroke Rehabilitation and Brain Recovery, Heidelberg, VIC, Australia.

[4] School of Biomedical Sciences and Pharmacy and the Priority Research Centre for Brain

and Mental Health Research, University of Newcastle, Callaghan, NSW, Australia.

[5] School of Electrical Engineering and Computer Science, University of Newcastle, Callaghan, NSW, Australia.

Corresponding Author

Frederick R. Walker

School of Biomedical Sciences and Pharmacy and the Priority Research Centre for Stroke and Brain Injury, University of Newcastle, Callaghan, NSW, Australia. Hunter Medical Research Institute, Newcastle, NSW, Australia.

E-mail: rohan.walker@newcastle.edu.au

Abstract

Exposure to psychological stress is known to seriously disrupt the operation of the substantia nigra (SN) and may in fact initiate the loss of dopaminergic neurons within the SN. In this study, we aimed to investigate how chronic stress modified the SN in adult male mice. Using a paradigm of repeated restraint stress (an average of 20 h per week for 6 weeks), we examined changes within the SN using a combination of western blotting and immunohistochemistry approaches. We demonstrated that chronic stress was associated with a clear loss of dopaminergic neurons within the SN. The loss of dopaminergic neurons was accompanied by higher levels of oxidative stress damage, indexed by levels of protein carbonylation and strong suppression of both microglial and astrocytic responses. In addition, we demonstrated for the first time that chronic stress alone enhanced the aggregation of α-synuclein into insoluble protein fraction. These results indicate that chronic stress triggered loss of dopaminergic neurons via increased level of oxidative stress, suppressed glia neuroprotective functions and enhanced the aggregation of the neurotoxic protein, α-synuclein. Collectively, these results reinforce the negative effects of chronic stress on the viability of dopaminergic cells with the SN.

Keywords:

α-synuclein; astrocytes; chronic stress; microglia; neurodegeneration; oxidative stress; substantia nigra.

1. Introduction

The substantia nigra (SN) is located within the midbrain and houses a dense population of dopaminergic neurons. This neuronal cell group is characterised by the expression of tyrosine hydroxylase (TH), the rate limiting enzyme in dopamine synthesis. The SN and associated sub-divisions has been the subject of extensive research due to the fact that the dopamine produced within the SN is essential in the control of motor function, and damage or degeneration of dopaminergic neurons within the SN is associated with movement pathologies.

Recently, it has been noted that psychological stress disrupts the normal operation of the SN and may in fact initiate the loss of dopaminergic neurons within the SN (Djamshidian and Lees, 2014; Herrera et al., 2015). Several studies in humans have shown that chronic stress could be considered as a risk factor in the development of movement pathologies, such as Parkinson's disease (Palhagen et al., 2008; Schuurman et al., 2002; Tanner et al., 2009). Preclinical studies undertaken using a variety of animal models of Parkinson's disease (6-hydroxydopamine, lipopolysaccharide, 1-methyl-4-phenyl-1,2,3,6-tetrahydropyridine) have shown that chronic stress accelerates the loss of TH positive neurons within the SN (de Pablos et al., 2014; Janakiraman et al., 2016; Lauretti et al., 2016; Smith et al., 2008). Particularly notable amongst recent reports, is a study by Sugama et al. (2016), which showed that rats exposed to chronic restraint stress exhibited significant loss of TH positive neurons within the SN after 2 weeks (~20 %), and continued loss after 16 weeks (~60 %) (Sugama et al., 2016). Interestingly, the authors suggested that the loss of TH positive neurons within the SN was associated with intense glial reactivity and generation of reactive oxygen species (ROS) (Sugama et al., 2016). On the basis of these results the authors proposed that chronic stress enhanced glial reactivity and associated ROS generation preceded the loss of

dopaminergic neurons (Herrera et al., 2015; McGeer and McGeer, 2008).

While the results presented by Sugama et al. (2016) are straightforward, there are increasing numbers of instances where results from studies done in rats do not align with the results obtained in mice and vice versa. We have noted that one area where mice and rats findings do not align well is in relation to how glia respond to chronic stress (Walker et al., 2013; Yirmiya et al., 2015). For instance, several comprehensive studies have consistently shown that chronic stress in rats is associated with increased levels of Iba1 (a microglial specific cytoskeletal protein) immunoreactivity (Hinwood et al., 2012; Hinwood et al., 2013; Kopp et al., 2013; Pan et al., 2014; Tynan et al., 2010). Chronic stress in mice, however, appears to cause an opposite change, with reductions in Iba1 immunoreactivity (Jones et al., 2015; Kreisel et al., 2014).

Given the differential impact of stress on microglia cytoskeletal remodelling in mice and rats we were interested in examining whether chronic stress in mice exerted the same detrimental effects on TH neurons within the SN (as have been reported in rats) and further examined signalling pathways that may be recruited in this process. Accordingly, in the current study we adopted a relatively simple approach, with a handled control group and another exposed to repeated restraint stress for 6 consecutive weeks. We first examined changes in the level of TH protein, the number of TH positive neurons and the density of TH immunoreactivity within the SN. Secondly, we examined changes in levels of oxidative stress within the SN, using protein carbonylation as an index of protein oxidation. We also examined changes in both microglia and astrocyte populations and a number of associated markers within the SN.

Further, a common hallmark of neurodegenerative diseases is the presence of proteinaceous

inclusion bodies caused by misfolded and intracellular aggregation of proteins in various brain regions. α-synuclein is known to be the main composition of Lewy bodies, which are found within the SN of patients with Parkinson's disease (Spillantini et al., 1997). The expression, regulation or pattern of α-synuclein have been extensively studied in animal models of Parkinson's disease (Giraldez-Perez et al., 2014; Maries et al., 2003). To our knowledge, no previous studies have examined whether exposure to chronic stress alone may alter the mechanisms of α-synuclein in the SN. Accordingly, in the current study we assessed the aggregation of α-synuclein within the SN.

2. Methods

2.1 Animals and treatments

All experiments were approved by the University of Newcastle Animal Care and Ethics Committee, and conducted in accordance with the New South Wales Animals Research Act and the Australian Code of Practice for the use of animals for scientific purposes. This study also complies with the ARRIVE guidelines. A total of 28 C57BL/6 adult male mice (8 weeks old) were each randomly allocated to a control or stress group (n=14 per group). Mice were obtained from the Animal Services Unit at the University of Newcastle. Mice were maintained in a temperature (21 °C ± 1) and humidity controlled environment with food and water available ad libitum. Lighting was on a 12:12 h reverse light–dark cycle (lights on 19:00 h) with all procedures conducted in the dark phase under low-level red lighting (40 Lux). Mice were allowed to acclimate for a minimum of seven days prior to the start of the experiment. Chronic stress was induced using a restraint stress model. Briefly, mice were placed in 50 mL conical tubes with ventilation holes for 2 h, 3 h, 4 h, 5 h or 6 h per day for 5 days per week randomly, an average of 20 h per week for 6 weeks in their home cage. The

variation in the duration of exposure and time of delivery ensures that the stress response is persistence. This restraint protocol is a well validated model, which has been shown to effectively induce stress-related behaviours in mice (Huang et al., 2015). Control mice had no access to food and water for the same period of time as stressed mice, and were handled for 2 min twice daily. All mice were weighted throughout the duration of experiment.

2.2 Tissue processing

Mice were sacrificed 6 weeks after the initiation of chronic stress treatment. For western blot analysis, mice (n=7 per group) were deeply anesthetized via intraperitoneal injection of sodium pentobarbitol and transcardially perfused with ice cold 0.9 % saline for 2 mins. Brains were dissected and rapidly frozen in -80˚C isopentane. Section were sliced in a cryostat (-20°C) at a thickness of 200 µm and SN (bregma -2.8 to -3.8 mm) were punched using a 2 mm tissue punch (Figure 2A). Substantia nigra samples were kept frozen at all times until protein extraction. For immunohistochemistry analysis, mice (n=7 per group) were deeply anesthetized via intraperitoneal injection of sodium pentobarbitol and transcardially perfused with ice cold 0.9 % saline for 2 mins followed by ice cold 4 % paraformaldehyde (pH 7.4) for 13 mins. Brains were removed and postfixed for 4 h in the same fixative then transferred to a 12.5 % sucrose solution in 0.1 M PBS for storage and cyroprotection. Serial coronal sections were sliced on a freezing microtome (-25°C) at a thickness of 30 µm and stored in cytoprotection solution at 4°C until analysis.

2.3 Protein extraction and western blot

Protein extraction and western blot were performed as previously described with minor modification (Ong et al., 2014). SN samples were sonicated in 300 µL of lysis buffer (50 mM TRIS pH 7.4, 1 mM EDTA, 1 mM DTT, 80 µM ammonium molybdate, 1 mM sodium

pyrophosphate, 1 mM sodium vanadate, 5 mM b-glycerolphosphate, 1 protease inhibitor cocktail tablet, 1 phosphatase inhibitor cocktail tablet, final concentration) with a UP50H microsonicator (Hielscher Ultrasonics GmbH, Germany) for 3 x 30 s pulses at 4°C. Samples were centrifuged at 14 000 g for 20 min at 4°C. The supernatant (soluble) fractions were collected and pellet (insoluble) fractions were resuspended in 100 µL of sodium dodecyl sulfate buffer (2 % sodium dodecyl sulfate, 50 mM Tris pH 7.4). Protein concentrations were determined by Pierce BCA protein assay kit (Thermo Fisher Scientific, USA) according to the manufacturer's instructions. Samples were diluted to equalize protein concentrations (1.5 mg/mL) and stored at -80°C until further analysis.

Samples were mixed with sample buffer (2 % sodium dodecyl sulfate, 50 mM Tris, 10 % glycerol, 1 % DTT, 0.1 % bromophenol blue, pH 6.8) and 15 µg of total tissue protein samples were electrophoresed to Biorad Criterion TGC Stain-Free 4-20 % gels. Gels were transferred to PVDF membranes by in transfer buffer (25 mM Tris, 200 mM glycine, 20 % methanol, pH 8.3). PVDF membranes were washed in Tris-buffered saline with tween (TBST) (150 mM NaCl, 10 mM Tris, 0.075% Tween-20, pH 7.5) and blocked in 5% skim milk powder in TBST for 1 h at 25°C. Membranes were incubated with primary antibodies for overnight at 4°C and secondary antibody for 1 h at 25°C (see Table 1 for antibodies concentration). In between each incubation step, membranes were washed in TBST. Membranes were visualized on an Amersham Imager 600 using Luminata Forte western blotting detection reagents. The density of the bands was measured using Amersham Imager 600 analysis software.

2.4 Oxidative damage to proteins (carbonyl)

The assessment of oxidative damage to proteins was determined by the OxiSelect Protein

Carbonyl Immunoblot Kit (Cell Biolabs Inc., CA, USA) according to the manufacturer's instruction. Briefly, 15 µg of total tissue protein samples were electrophoresed and transferred to PVDF membranes as described above. The protein carbonyl groups were then derivatized with dinitrophenylhydrazine on the membranes, followed by the incubation and wash steps mentioned above.

2.5 Immunohistochemistry

For immunoperoxidase labelling, free-floating sections were immunostained as previously described with minor modification (Tynan et al., 2010). All reactions were run at the same time, with the same reagents, at the same concentrations, by an experimenter blind to treatment. Briefly, all brain sections were incubated with 1 % hydrogen peroxidase for 30 min at 25˚C to quench endogenous peroxidase activity and were then incubated with 3 % horse serum for 30 min at 25˚C to block non-specific binding. Brain sections were incubated with primary antibody for 48 h at 4˚C and followed by secondary antibody for 1 h at 25˚C (see Table 1 for antibodies concentration). Next, brain sections were incubated for 2 h at 25˚C with avidin–biotin-peroxidase complex and then developed using DAB peroxidase substrate. Brain sections were washed with PBS in between each incubation step. After processing was complete, sections were mounted onto chrome alum-coated slides, and cover slipped.

2.6 Image acquisition, cell count and threshold analysis

Brain regions were identified by reference to the Mouse Brain in Stereotaxic Coordinates (Paxinos and Franklin, 2001). Images were acquired at 20 X using Aperio AT2 (Leica, Germany). Mosaic images were acquired and the SN at bregma level -3.3 mm were identified. Manual blinded cell counts within the SN were obtained for dopaminergic neurons

using TH, microglia using Iba1, astrocytes using GFAP and mature neurons using NeuN. The threshold analysis was evaluated as previously described (Jones et al., 2015; Ong et al., 2016; Patience et al., 2015). Briefly, Matlab software R2015a was used to crop SN from the mosaics. A pixel intensity level considered to be optimal for detecting genuine differences in immunoreactive signal was determined using ImageJ software to visualize thresholding of cropped regions at individual pixel intensities. This threshold level was used to investigate group differences for all labels.

2.7 Data analysis

All data for control and stress groups were expressed as percentage change relative to the average of control ± SEM (except for the changes (delta, Δ) of body weight) and were analyzed using Prism 6 for Windows Version 6.01, GraphPad Software. Unpaired t-test (two-tailed) was used to determine whether there were any significant effect between control and stress groups. Two-Way ANOVA was used to analyse percentage weight change. Additional Sidak post tests were used to analyse differences between the control and stress groups, where an overall stress treatment was found. The data were considered to be significant at $p < 0.05$ and shown on the graphs with asterisks (*).

3. Results

3.1 Chronic stress reduced weight gain

In order to assess the efficacy of our chronic stress paradigm, we measured the weekly change in body weight. The baseline body weight is 27.52 ± 0.50 g (minimum = 25.10 g; maximum = 30.50 g). The changes (delta, Δ) of body weight from baseline are shown in Figure 1. There was a significant effect of stress ($F_{(6, 36)} = 12.38$, $p < 0.001$) and time ($F_{(1, 6)} =$

45.70, $p < 0.01$) on the % weight change. Post hoc analysis indicated that stress caused a significant decrease in body weight relative to control group from 1 to 6 weeks.

3.2 Chronic stress induced the loss of dopaminergic neurons within the SN

The protein homogenates for western blot analysis were taken across the full extent of SN and were used to assess precise differences in TH protein (or other markers discussed below) between groups (Figure 2A). Representative immunoblots are shown in Figure 2B and the results for TH protein levels were normalized to β-actin as loading control. We found a significant decrease in TH protein levels in the stressed mice compared to controls (61 % vs 100 %, $p < 0.05$, Figure 2C).

Immunohistochemistry staining of TH antibodies (or other markers discussed below) was used at a single level of the SN (bregma level -3.3 mm) to validate western blot results and to better understand the spatial distribution of TH positive neurons (Figure 2D). We found a significant decrease in TH positive neurons in the stressed mice compared to controls (77 % vs 100 %, $p < 0.05$, Figure 2E).

Optical density of TH staining (and other staining discussed below) at the SN was then semi-quantitatively assessed using threshold analysis. Using ImageJ software, we identified that pixel intensity 144 detected genuine TH immunoreactive material (Figure 2F). The number of pixels that were captured at and below pixel intensity 144 was then expressed as a percentage of the total number of pixels in each image and these data were used to investigate between-group differences. We found a significant decrease in TH immunoreactive levels in the stressed mice compared to controls (56 % vs 100 %, $p < 0.01$, Figure 2G).

3.4 Chronic stress enhanced the levels of oxidative stress within the SN

Protein carbonylation is the most robust and commonly used marker for protein oxidation by oxidative stress. Briefly, the protein carbonyl groups on the electrophoresed protein homogenates were derivatized with dinitrophenylhydrazine on the membranes and probed with anti-DNP. Protein carbonylation immunoblots appeared as multiple bands (Figure 3A). We found a number of individual proteins which showed major changes in protein carbonylation within the SN of stressed mice, which was not in the control mice. The results for protein carbonylation levels (quantified as optical density of all bands for each lane) were normalized to β-actin levels. We found a significant increase in protein carbonyl levels in the stressed mice compared to controls (166 % vs 100 %, $p < 0.001$, Figure 3B).

3.4 Chronic stress reduced the levels of microglial activation markers within the SN

We analysed microglial complement receptor (CD11b), fractalkine receptor (CX3CR1) and cytoskeletal marker (Iba1) by western blot (Figure 4A). The results for CD11b, CX3CR1 and Iba1 were normalized to β-actin levels. We found a significant decrease in CX3CR1 and Iba1 protein levels in the stressed mice compared to controls (CX3CR1, 76 % vs 100 %, $p < 0.01$; Iba1, 79 % vs 100 %, $p < 0.05$, Figure 4C & 4D). We further confirmed the protein data using immunohistochemistry staining (Figure 4E), and found a significant decrease in Iba1 positive cells (91 % vs 100 %, $p < 0.001$, Figure 4F) and a significant decrease in Iba1 immunoreactive levels in the stressed mice compared to controls (66 % vs 100 %, $p < 0.05$, Figure 4G).

3.5 Chronic stress reduced the levels of astrocyte activation markers within the SN

We analysed astrocyte markers (Aldh1L1, GFAP and S100β) by western blot (Figure 5A). The results for Aldh1L1, GFAP and S100β were normalized to β-actin levels. We found a

significant decrease in GFAP and S100β protein levels in the stressed mice compared to controls (GFAP, 79 % vs 100 %, $p < 0.05$; S100β, 80 % vs 100 %, $p < 0.05$, Figure 5C & 5D). We further confirmed the protein data using immunohistochemistry staining (Figure 5E), and found a significant decreases in the number of GFAP positive cells (57 % vs 100 %, $p < 0.001$, Figure 5F) and a significant decreases in GFAP immunoreactive levels in the stressed mice compared to controls (74 % vs 100 %, $p < 0.05$, Figure 5G).

3.6 Chronic stress increased the aggregation of α-synuclein protein

The supernatant and pellet fractions were analysed by western blot for the levels of soluble and insoluble α-synuclein (Figure 6A). The results for α-synuclein monomer and dimer levels were normalized to β-actin levels. We found a significant decrease in soluble α-synuclein monomer levels, and a corresponding significant increase in insoluble α-synuclein monomer levels in the stressed mice compared to controls (soluble α-synuclein monomer, 81 % vs 100 %, $p < 0.05$; insoluble α-synuclein monomer, 144 % vs 100 %, $p < 0.05$, Figure 6B). Qualitatively, using high magnification images we found granulated α-synuclein staining distributed within the SN of stressed mice, which was not apparent in the control mice (Figure 6C).

4. Discussion

The primary aim of the current study was to examine how chronic stress in mice influenced the viability of dopaminergic neurons within the SN. Firstly, we showed that repeated restraint stress was associated with a clear reduction in the levels of TH protein, the number of TH positive neurons and the density of TH immunoreactivity, indicating a clear loss of dopaminergic neurons. Assessments of protein carbonylation, a surrogate marker for the

effect of oxidative stress, indicated that chronic stress was associated with significantly higher levels of oxidative stress damage. These results align perfectly with findings recently reported (Sugama et al., 2016). Secondly, we examined a variety of markers that are used as metrics of micro- and astro-gliosis. In contrast to previous results in rats by Sugama et al. (2016), we found that chronic stress in mice was associated with strong suppression of the both microglial and astrocyte responses. Thirdly, we demonstrated that chronic stress enhanced the aggregation of α-synuclein to the insoluble protein fraction. Collectively, the results from our study reinforce the negative effects of chronic stress on the viability of dopaminergic cells within the SN. However, it appears that the specific contribution of glia, and in turn how they could be therapeutically manipulated, requires further investigation.

We observed that repeated restraint stress is associated with the loss of dopaminergic neurons. Specifically, we investigated dopaminergic neurons and mature neurons within the SN using TH and NeuN respectively as markers. We found that there was a significant decrease in TH positive neurons, but not NeuN positive neurons (see Supplement Figure 1). There are two possible interpretations of this result. Firstly, repeated restraint stress may have decreased TH expression but not actual neuronal cell loss within the SN. Secondly, repeated restraint stress may have induced a preferential loss of TH positive neurons within the SN. The latter interpretation is closely align with recently reported findings from rats that repeated restraint stress induced the specific loss of dopaminergic neurons within the SN (Sugama et al., 2016). We and Sugama et al. (2016) also identified that exposure to repeated restraint stress results in higher levels of ROS activity, as indexed by levels of protein carbonylation in our study. We observed that repeated restraint stress alters protein carbonylation in a number of individual proteins. At this point we cannot precisely determine the cellular source of the ROS species. Kim et al. (2005) has reported that repeated restraint

stress can cause overproduction of endogenous dopamine, leading to dopamine breakdown and generation of ROS, which increase the vulnerability of the neurons within the SN (Kim et al., 2005). In contrast, Sugama et al. (2016) suggested that chronic stress-enhanced glial reactivity was the primary driver for enhanced ROS generation and subsequent loss of dopaminergic neurons (Sugama et al., 2016). Therefore, it would be of interest in future to examine the primary cellular source of the ROS species seen in the SN after chronic stress.

Where the results of current study diverge from the previous rat-based study undertaken by Sugama et al. (2016) is in relation to the chronic stress induced microglial changes. We observed that repeated restraint stress in mice was associated with a reduction in the microglial cytoskeletal marker, Iba1 (rather than enhancement shown in rats), a reduction in the fractalkine receptor, CX3CR1, with no changes being observed in the expression of integrin complement receptor, CD11b. In attempting to resolve the discrepancy, perhaps the most obvious difference between our experimental approach and that of Sugama et al. (2016) is the choice of species, with male C57BL/6 mice being used in our study versus male Wistar rats in the other study. A closer examination of the literature concerning the effects of chronic stress on microglia appears to confirm that species differences may in fact exist (Walker et al., 2013; Yirmiya et al., 2015). For instance, most of the early studies to examine the effects of chronic stress were done in rats and observed that chronic stress enhanced the expression of Iba1, structural marker for the microglial cytoskeleton (Hinwood et al., 2012; Kopp et al., 2013; Tynan et al., 2010). These results have been commonly interpreted as indicating that microglia had become more pro-inflammatory and contributed to a less favourable environment for neuronal survival. Several recent studies have examined the effects of chronic stress in mice and reported that chronic stress reduced the size of microglia soma and diminished the expression of Iba1 (Jones et al., 2015; Kreisel et al., 2014; Milior et al., 2016).

These results could be interpreted as suppression of microglial neuroprotective functions, in particular the anti-inflammatory actions. Further phenotyping studies on microglia using classical microglial pro-inflammatory activation markers, M1 (such as MHCII, CD45, CD68) and alternate microglial anti-inflammatory markers, M2 (such as Arg-1, Ym-1, CD206) are warranted. The issue of whether microglial function is enhanced or suppressed by chronic stress is a significant one (Herrera et al., 2015), as it has the potential to make a major difference the type of therapeutic interventions pursued to limit chronic stress-induced loss of dopaminergic neurons within the SN.

We further observed that repeated restraint stress in mice was associated with a reduction in the astroglial cytoskeletal markers, GFAP, a reduction in the calcium binding protein S100β produced by astrocytes, with no changes being observed in the expression of Aldh1L1, an astrocyte specific protein involved in astrocyte metabolism. Interestingly, our findings in mice with respect to astrocytes are relatively consistent with those reported in rats that chronic stress is associated with robust down-regulation of GFAP (Gosselin et al., 2009; Imbe et al., 2012; Saur et al., 2016; Tynan et al., 2013). Based on the evidence, it had become widely accepted that chronic stress induces a significant disruption in astrocyte function and that this disruption is pivotal to the observed neuronal disturbances.

We also investigated whether exposure to repeated restraint stress altered the aggregation of α-synuclein within the SN. α-synuclein is a natively soluble unfolded protein, which undergoes spontaneous aggregation under different environmental conditions (Breydo et al., 2012). While the precise function of α-synuclein remains equivocal, evidence suggests that the insoluble form of α-synuclein may be responsible for cellular dysfunction (Campbell et al., 2000; Leong et al., 2009; Winner et al., 2011). To investigate the aggregation of α-

synuclein, we analysed both soluble and insoluble protein fractions using SDS-PAGE in combination with western blotting. The advantage of this approach is that it provides direct measurement on the relative levels of soluble and insoluble α-synuclein. We observed that repeated restraint stress in mice was associated with a reduction in soluble α-synuclein levels and a corresponding enhancement in insoluble α-synuclein levels within the SN. We further confirmed this observation using immunohistochemistry, which revealed increased immunostaining of α-synuclein punctae in the SN. The changes in the solubility status of α-synuclein may be driven by enhanced level of oxidative stress (Curtis et al., 2012; Leong et al., 2009), we however did not address this relationship directly.

In conclusion, the effect of chronic stress on the integrity of the SN has attracted considerable interest due to the possibility that chronic stress makes the SN more vulnerable to degeneration and therefore acts as a risk factor in the emergence of SN linked pathologies, such as Parkinson's diseases (Djamshidian and Lees, 2014; Herrera et al., 2015). The current study was undertaken in order to better understand how exposure to repeated restraint stress altered the SN in adult male mice. In addition to being the first study to confirm that chronic stress drives loss of TH neurons within the SN, it is also first to demonstrated chronic stress-induced enhancement of the aggregation of α-synuclein. We have also identified that chronic stress may drive these changes through oxidative stress damage. However, the suppression of glial responses raises important questions around how significant the contribution of these cells are to the loss of dopaminergic neurons within the SN. Certainly, future detailed phenotyping of glial cells within the SN is warranted.

Acknowledgments

The authors disclosed receipt of the following financial support for the research, authorship

and/or publication of this article. This study was part supported by the Hunter Medical Research Institute (HMRI 15-42), Faculty of Health and Medicine Pilot Grant and The University of Newcastle, Australia. We would like to thank International Brain Research Organization (IBRO) for supporting LKO with Young Investigator Travel Program. We express our gratitude to Dr Rick Thorne and HMRI Core Histology Facility for assistance with the immunohistochemistry images.

Declaration of conflicting interests

The authors declared no potential conflicts of interest with respect to the research, authorship, and/or publication of this article.

Authors' contributions

LKO and FRW designed the experiment. ZZ performed the animal experiments and prepared the brain sections. LKO performed majority of the western blot and immunohistochemistry experiments. LKO and MK provided antibodies optimization and quality control of the western blot protocol. SJJ designed and prepared program for the image processing. ZZ, CT and KZ performed image acquisition, blind cell count and threshold analysis. LKO and FRW analysed the data, interpreted the results and wrote the manuscript. ZZ, MK, PWD, SJJ and MN helped results interpretation and revise the manuscript.

References

Breydo, L., Wu, J.W., Uversky, V.N., 2012. Alpha-synuclein misfolding and Parkinson's disease. Biochim Biophys Acta 1822, 261-285.

Campbell, B.C., Li, Q.X., Culvenor, J.G., Jakala, P., Cappai, R., Beyreuther, K., Masters, C.L., McLean, C.A., 2000. Accumulation of insoluble alpha-synuclein in dementia with Lewy bodies. Neurobiol Dis 7, 192-200.

Curtis, J.M., Hahn, W.S., Long, E.K., Burrill, J.S., Arriaga, E.A., Bernlohr, D.A., 2012. Protein carbonylation and metabolic control systems. Trends Endocrinol Metab 23, 399-406.

de Pablos, R.M., Herrera, A.J., Espinosa-Oliva, A.M., Sarmiento, M., Munoz, M.F., Machado, A., Venero, J.L., 2014. Chronic stress enhances microglia activation and exacerbates death of nigral dopaminergic neurons under conditions of inflammation. J Neuroinflammation 11, 34.

Djamshidian, A., Lees, A.J., 2014. Can stress trigger Parkinson's disease? J Neurol Neurosurg Psychiatry 85, 878-881.

Giraldez-Perez, R., Antolin-Vallespin, M., Munoz, M., Sanchez-Capelo, A., 2014. Models of alpha-synuclein aggregation in Parkinson's disease. Acta Neuropathol Commun 2, 176.

Gordon, S.L., Bobrovskaya, L., Dunkley, P.R., Dickson, P.W., 2009. Differential regulation of human tyrosine hydroxylase isoforms 1 and 2 in situ: Isoform 2 is not phosphorylated at Ser35. Biochim Biophys Acta 1793, 1860-1867.

Gosselin, R.D., Gibney, S., O'Malley, D., Dinan, T.G., Cryan, J.F., 2009. Region specific decrease in glial fibrillary acidic protein immunoreactivity in the brain of a rat model of depression. Neuroscience 159, 915-925.

Herrera, A.J., Espinosa-Oliva, A.M., Carrillo-Jimenez, A., Oliva-Martin, M.J., Garcia-Revilla, J., Garcia-Quintanilla, A., de Pablos, R.M., Venero, J.L., 2015. Relevance of chronic stress and the two faces of microglia in Parkinson's disease. Front Cell Neurosci 9, 312.

Hinwood, M., Morandini, J., Day, T.A., Walker, F.R., 2012. Evidence that microglia mediate the neurobiological effects of chronic psychological stress on the medial prefrontal cortex. Cereb Cortex 22, 1442-1454.

Hinwood, M., Tynan, R.J., Charnley, J.L., Beynon, S.B., Day, T.A., Walker, F.R., 2013. Chronic stress induced remodeling of the prefrontal cortex: structural re-organization of microglia and the inhibitory effect of minocycline. Cereb Cortex 23, 1784-1797.

Huang, R.R., Hu, W., Yin, Y.Y., Wang, Y.C., Li, W.P., Li, W.Z., 2015. Chronic restraint stress promotes learning and memory impairment due to enhanced neuronal endoplasmic reticulum stress in the frontal cortex and hippocampus in male mice. Int J Mol Med 35, 553-559.

Imbe, H., Kimura, A., Donishi, T., Kaneoke, Y., 2012. Chronic restraint stress decreases glial fibrillary acidic protein and glutamate transporter in the periaqueductal gray matter. Neuroscience 223, 209-218.

Janakiraman, U., Manivasagam, T., Thenmozhi, A.J., Essa, M.M., Barathidasan, R., SaravanaBabu, C., Guillemin, G.J., Khan, M.A., 2016. Influences of Chronic Mild Stress Exposure on Motor, Non-Motor Impairments and Neurochemical Variables in Specific Brain Areas of MPTP/Probenecid Induced Neurotoxicity in Mice. PLoS One 11, e0146671.

Jones, K.A., Zouikr, I., Patience, M., Clarkson, A.N., Isgaard, J., Johnson, S.J., Spratt, N., Nilsson, M., Walker, F.R., 2015. Chronic stress exacerbates neuronal loss associated with secondary neurodegeneration and suppresses microglial-like cells following focal motor cortex ischemia in the mouse. Brain Behav Immun 48, 57-67.

Kim, S.T., Choi, J.H., Chang, J.W., Kim, S.W., Hwang, O., 2005. Immobilization stress causes increases in tetrahydrobiopterin, dopamine, and neuromelanin and oxidative damage in the nigrostriatal system. J Neurochem 95, 89-98.

Kopp, B.L., Wick, D., Herman, J.P., 2013. Differential effects of homotypic vs. heterotypic chronic stress regimens on microglial activation in the prefrontal cortex. Physiol Behav 122, 246-252.

Kreisel, T., Frank, M.G., Licht, T., Reshef, R., Ben-Menachem-Zidon, O., Baratta, M.V., Maier, S.F., Yirmiya, R., 2014. Dynamic microglial alterations underlie stress-induced depressive-like behavior and suppressed neurogenesis. Mol Psychiatry 19, 699-709.

Lauretti, E., Di Meco, A., Merali, S., Pratico, D., 2016. Chronic behavioral stress exaggerates motor deficit and neuroinflammation in the MPTP mouse model of Parkinson's disease. Transl Psychiatry 6, e733.

Leong, S.L., Cappai, R., Barnham, K.J., Pham, C.L., 2009. Modulation of alpha-synuclein aggregation by dopamine: a review. Neurochem Res 34, 1838-1846.

Maries, E., Dass, B., Collier, T.J., Kordower, J.H., Steece-Collier, K., 2003. The role of alpha-synuclein in Parkinson's disease: insights from animal models. Nat Rev Neurosci 4, 727-738.

McGeer, P.L., McGeer, E.G., 2008. Glial reactions in Parkinson's disease. Mov Disord 23, 474-483.

Milior, G., Lecours, C., Samson, L., Bisht, K., Poggini, S., Pagani, F., Deflorio, C., Lauro, C., Alboni, S., Limatola, C., Branchi, I., Tremblay, M.E., Maggi, L., 2016. Fractalkine receptor deficiency impairs microglial and neuronal responsiveness to chronic stress. Brain Behav Immun 55, 114-125.

Ong, L.K., Guan, L., Damanhuri, H., Goodchild, A.K., Bobrovskaya, L., Dickson, P.W., Dunkley, P.R., 2014. Neurobiological consequences of acute footshock stress: effects on tyrosine hydroxylase phosphorylation and activation in the rat brain and adrenal medulla. J Neurochem 128, 547-560.

Ong, L.K., Zhao, Z., Kluge, M., Walker, F.R., Nilsson, M., 2016. Chronic stress exposure following photothrombotic stroke is associated with increased levels of Amyloid beta accumulation and altered oligomerisation at sites of thalamic secondary neurodegeneration in mice. Journal of Cerebral Blood Flow & Metabolism.

Palhagen, S.E., Carlsson, M., Curman, E., Walinder, J., Granerus, A.K., 2008. Depressive illness in Parkinson's disease--indication of a more advanced and widespread neurodegenerative process? Acta Neurol Scand 117, 295-304.

Pan, Y., Chen, X.Y., Zhang, Q.Y., Kong, L.D., 2014. Microglial NLRP3 inflammasome activation mediates IL-1beta-related inflammation in prefrontal cortex of depressive rats. Brain Behav Immun 41, 90-100.

Patience, M.J., Zouikr, I., Jones, K., Clarkson, A.N., Isgaard, J., Johnson, S.J., Walker, F.R., Nilsson, M., 2015. Photothrombotic stroke induces persistent ipsilateral and contralateral astrogliosis in key cognitive control nuclei. Neurochem Res 40, 362-371.

Paxinos, G., Franklin, K.B.J., 2001. The mouse brain in stereotaxic coordinates. Academic Press, San Diego.

Saur, L., Baptista, P.P., Bagatini, P.B., Neves, L.T., de Oliveira, R.M., Vaz, S.P., Ferreira, K., Machado, S.A., Mestriner, R.G., Xavier, L.L., 2016. Experimental Post-traumatic Stress Disorder Decreases Astrocyte Density and Changes Astrocytic Polarity in the CA1 Hippocampus of Male Rats. Neurochem Res 41, 892-904.

Schuurman, A.G., van den Akker, M., Ensinck, K.T., Metsemakers, J.F., Knottnerus, J.A., Leentjens, A.F., Buntinx, F., 2002. Increased risk of Parkinson's disease after depression: a retrospective cohort study. Neurology 58, 1501-1504.

Smith, L.K., Jadavji, N.M., Colwell, K.L., Katrina Perehudoff, S., Metz, G.A., 2008. Stress accelerates neural degeneration and exaggerates motor symptoms in a rat model of Parkinson's disease. Eur J Neurosci 27, 2133-2146.

Spillantini, M.G., Schmidt, M.L., Lee, V.M., Trojanowski, J.Q., Jakes, R., Goedert, M., 1997. Alpha-synuclein in Lewy bodies. Nature 388, 839-840.

Sugama, S., Sekiyama, K., Kodama, T., Takamatsu, Y., Takenouchi, T., Hashimoto, M., Bruno, C., Kakinuma, Y., 2016. Chronic restraint stress triggers dopaminergic and noradrenergic neurodegeneration: Possible role of chronic stress in the onset of Parkinson's disease. Brain Behav Immun 51, 39-46.

Tanner, C.M., Ross, G.W., Jewell, S.A., Hauser, R.A., Jankovic, J., Factor, S.A., Bressman, S., Deligtisch, A., Marras, C., Lyons, K.E., Bhudhikanok, G.S., Roucoux, D.F., Meng, C., Abbott, R.D., Langston, J.W., 2009. Occupation and risk of parkinsonism: a multicenter case-control study. Arch Neurol 66, 1106-1113.

Tynan, R.J., Beynon, S.B., Hinwood, M., Johnson, S.J., Nilsson, M., Woods, J.J., Walker, F.R., 2013. Chronic stress-induced disruption of the astrocyte network is driven by structural atrophy and not loss of astrocytes. Acta Neuropathol 126, 75-91.

Tynan, R.J., Naicker, S., Hinwood, M., Nalivaiko, E., Buller, K.M., Pow, D.V., Day, T.A., Walker, F.R., 2010. Chronic stress alters the density and morphology of microglia in a subset of stress-responsive brain regions. Brain Behav Immun 24, 1058-1068.

Walker, F.R., Nilsson, M., Jones, K., 2013. Acute and chronic stress-induced disturbances of microglial plasticity, phenotype and function. Curr Drug Targets 14, 1262-1276.

Winner, B., Jappelli, R., Maji, S.K., Desplats, P.A., Boyer, L., Aigner, S., Hetzer, C., Loher, T., Vilar, M., Campioni, S., Tzitzilonis, C., Soragni, A., Jessberger, S., Mira, H., Consiglio, A., Pham, E., Masliah, E., Gage, F.H., Riek, R., 2011. In vivo demonstration that alpha-synuclein oligomers are toxic. Proc Natl Acad Sci U S A 108, 4194-4199.

Yirmiya, R., Rimmerman, N., Reshef, R., 2015. Depression as a microglial disease. Trends Neurosci 38, 637-658.

Legends

Figure 1. Chronic restraint stress significantly reduced body weight gain. Delta (Δ) body weight change from baseline with the differences expressed in gram (g).

Figure 2. Chronic restraint stress induced specific loss of dopaminergic neurons at the SN. A. SN tissues (in red shade) were dissected from fresh frozen brain at bregma -2.8 to -3.8 for protein analysis by western blotting. Western blot results were then validated with fixed tissues at a single level bregma -3.3 by immunohistochemistry staining. B. Representative immunoblots for TH and β-actin of the SN comparing the effects of control and stress. C. The results for TH protein levels were calculated relative to β-actin levels. Chronic stress significantly reduced TH protein levels. D. TH immunostaining in the SN. E. Chronic stress significantly reduced TH positive cells. F. TH staining (left panels) and the material thresholded at pixel intensity (PI) 144 (right panels) of the SN. G. Chronic stress significantly reduced thresholded TH staining at pixel intensity 144.

Figure 3. Protein carbonylation in the SN following chronic restraint stress. A. Representative immunoblots for DNP and β-actin of the SN comparing the effects of control and stress. B. Chronic restraint stress significantly increased DNP (protein carbonylation) levels.

Figure 4. Microglia markers following chronic restraint stress. A. Representative immunoblots for CD11b, CX3CR1, Iba1 and β-actin from the SN comparing the effects of control and stress. The results for CD11b, CX3CR1 and Iba1 levels were calculated relative to β-actin levels. B. There was no significant change in CD11b levels. Chronic stress

significantly reduced C. CX3CR1 and D. Iba1 levels. E. Iba1 staining (left panels) and the material thresholded at pixel intensity (PI) 159 (right panels) of the SN. F. Chronic stress significantly reduced Iba1 positive cells. G. Chronic stress significantly reduced thresholded Iba1 staining at pixel intensity 159.

Figure 5. Astrocytes markers following chronic restraint stress. A. Representative immunoblots for ALDH1L1, GFAP, S100β and β-actin from the SN comparing the effects of control and stress. The results for ALDH1L1, GFAP and S100β levels were calculated relative to β-actin levels. B. There was no significant change in ALDH1L1 levels. Chronic stress significantly reduced C. GFAP and D. S100β levels. E. GFAP staining (left panels) and the material thresholded at pixel intensity (PI) 108 (right panels) of the SN. F. Chronic stress significantly reduced GFAP positive cells. G. Chronic stress significantly reduced thresholded GFAP staining at pixel intensity 108.

Figure 6. Aggregation of α-synuclein in the SN following chronic restraint stress. A. Representative immunoblots for α-synuclein and β-actin of the SN soluble and insoluble fractions comparing the effects of control and stress. B. Chronic restraint stress significantly reduced soluble α-synuclein monomer levels, but significantly increased insoluble α-synuclein monomer levels. C. High magnifying images depicted that chronic stress significantly increased immunostaining of α-synuclein punctae (white arrows) in the SN. Bottom high magnifying (40X) images were directly obtained (marked, X) from top low magnifying (10x) images.

Table and Figures

Table 1: List of antibodies used for western blot and immunohistochemistry analyses.

Target	Sources of antibodies	Application	Dilution
TH	Total TH antibody*	WB	1:5000
		IHC	1:7500
DNP	Cell Biolabs Inc, Anti-DNP Antibody, STA-308	WB	1:3000
CD11b	Abcam, Anti-CD11b antibody, ab75476	WB	1:2000
CX3CR1	Abcam, Anti-CX3CR1 antibody, ab8021	WB	1:2000
Iba1	Abcam, Anti-Iba1 antibody, ab5076	WB	1:2000
	Wako, Anti-Iba1 antibody, #019-19741	IHC	1:1000
ALDH1L1	Millipore, Anti-ALDH1L1 antibody, MABN495	WB	1:2000
GFAP	Cell Signaling, Anti-GFAP antibody, #3670	WB	1:5000
	Sigma, Anti-GFAP antibody, G3893	IHC	1:1500
S100β	Cell Signaling, Anti- S100β antibody, #9550	WB	1:1000
α-synuclein	BD Biosciences, Anti-α-Synuclein antibody, #610787	WB	1:1000
		IHC	1:500
β-actin	Sigma-Aldrich, Monoclonal Anti-β-actin-HRP antibody, A3854	WB	1:50000
Rabbit IgG	Biorad, Anti-Rabbit-HRP antibody, #170-6515	WB	1:5000
	Jackson ImmunoReseach, Anti-Rabbit-Biotin, #111-065-003	IHC	1:500
Mouse IgG	Biorad, Anti-Mouse-HRP antibody, #170-6516	WB	1:10000
	Jackson ImmunoReseach, Anti-Mouse-Biotin, #115-065-003	IHC	1:500
Goat IgG	Santa Cruz, Anti-Goat-HRP antibody, sc-2020	WB	1:5000

WB, western blot; IHC, immunohistochemistry. *Antibodies were generated and tested for specificity as described (Gordon et al., 2009).

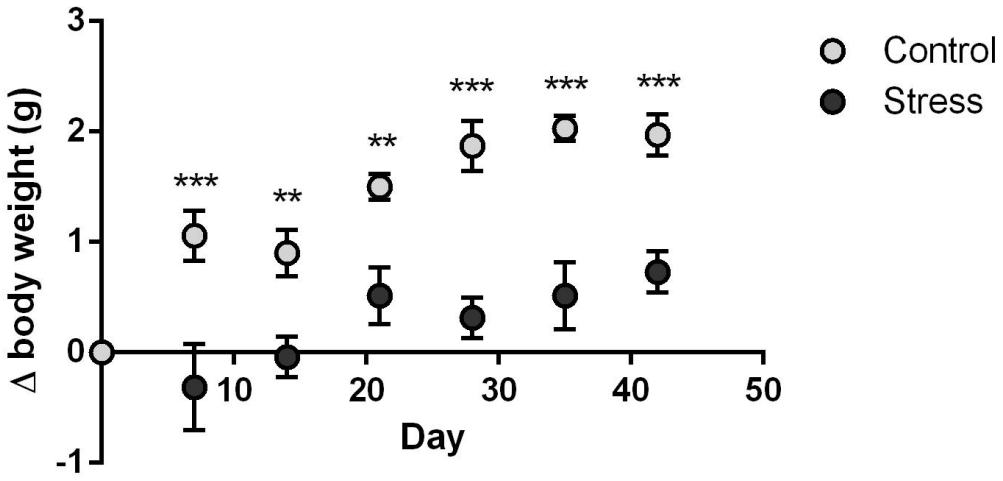

Figure 1.

Chronic restraint stress significantly reduced body weight gain. Delta (Δ) body weight change from baseline with the differences expressed in gram (g).

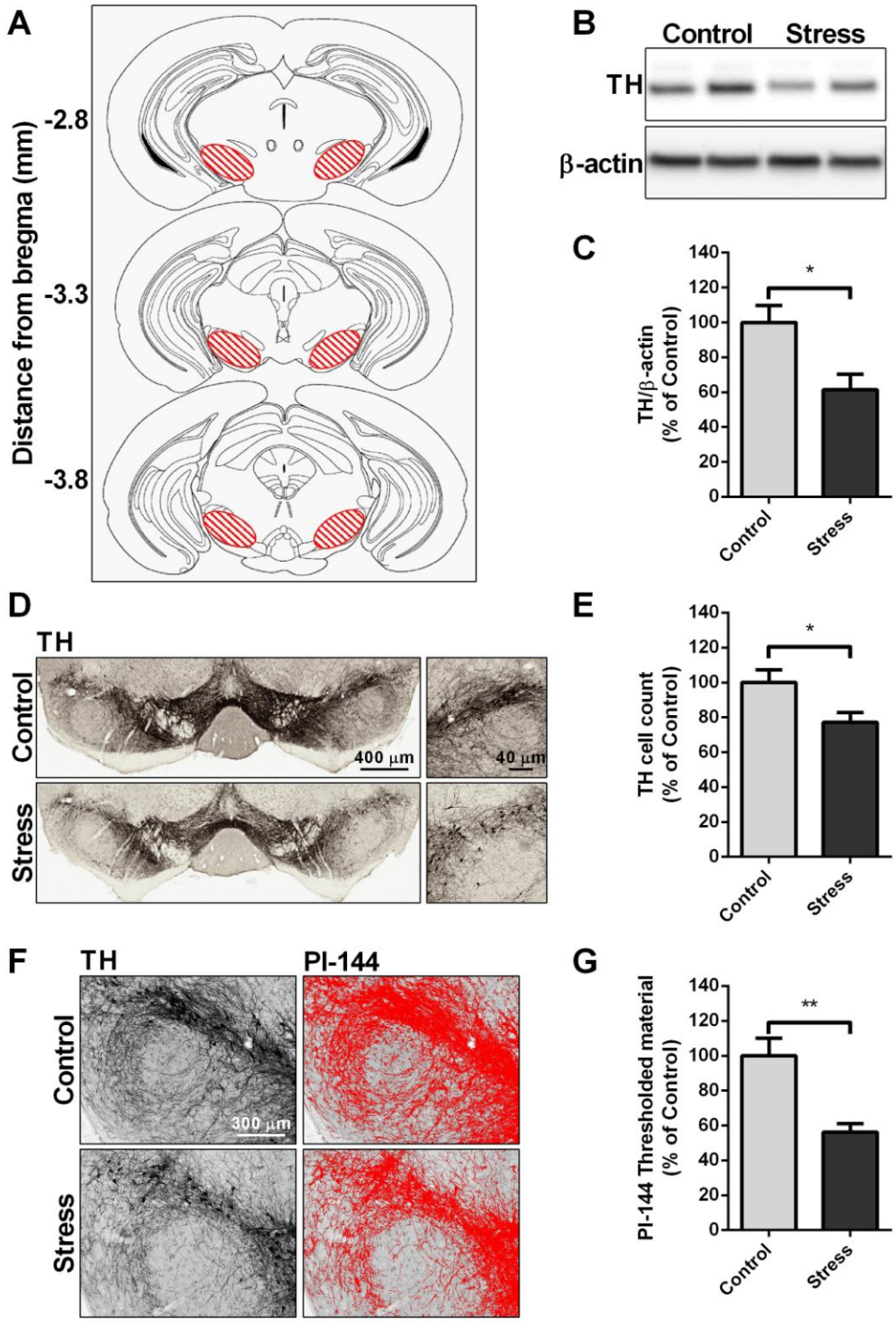

Figure 2.

Chronic restraint stress induced specific loss of dopaminergic neurons at the SN. A. SN tissues (in red shade) were dissected from fresh frozen brain at bregma -2.8 to -3.8 for protein analysis by western blotting. Western blot results were then validated with fixed tissues at a

single level bregma -3.3 by immunohistochemistry staining. B. Representative immunoblots for TH and β-actin of the SN comparing the effects of control and stress. C. The results for TH protein levels were calculated relative to β-actin levels. Chronic stress significantly reduced TH protein levels. D. TH immunostaining in the SN. E. Chronic stress significantly reduced TH positive cells. F. TH staining (left panels) and the material thresholded at pixel intensity (PI) 144 (right panels) of the SN. G. Chronic stress significantly reduced thresholded TH staining at pixel intensity 144.

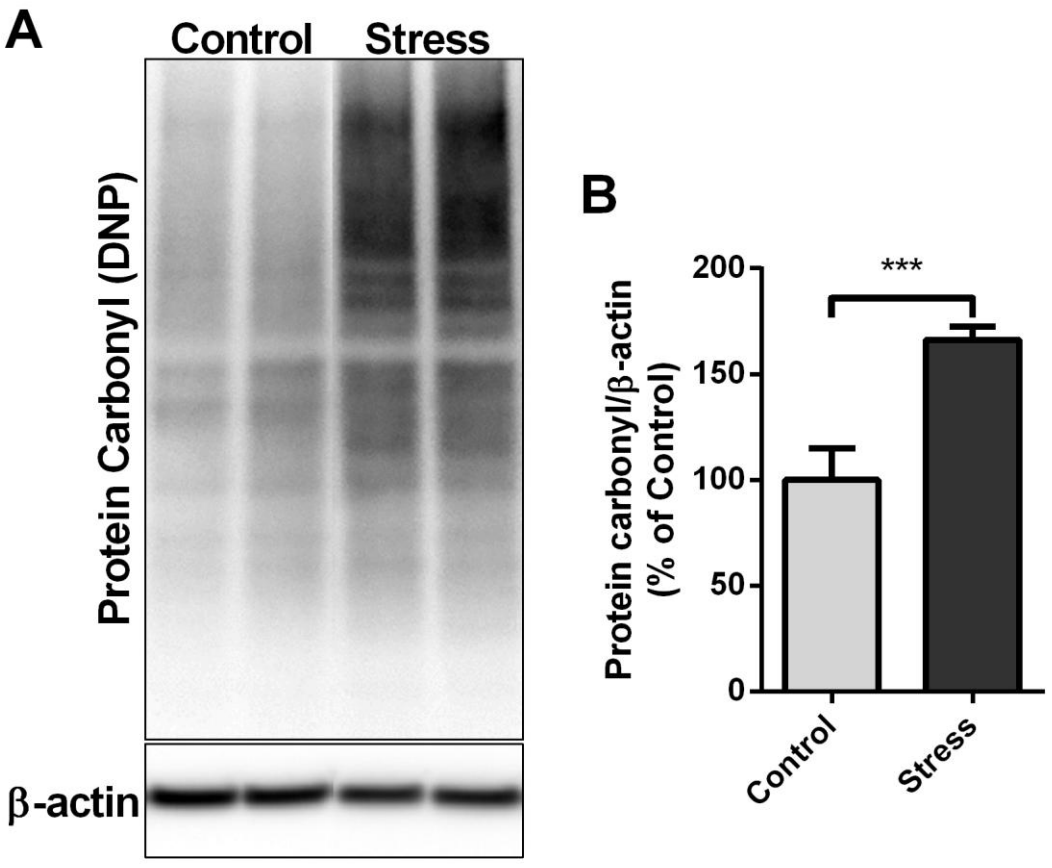

Figure 3.

Protein carbonylation in the SN following chronic restraint stress. A. Representative immunoblots for DNP and β-actin of the SN comparing the effects of control and stress. B. Chronic restraint stress significantly increased DNP (protein carbonylation) levels.

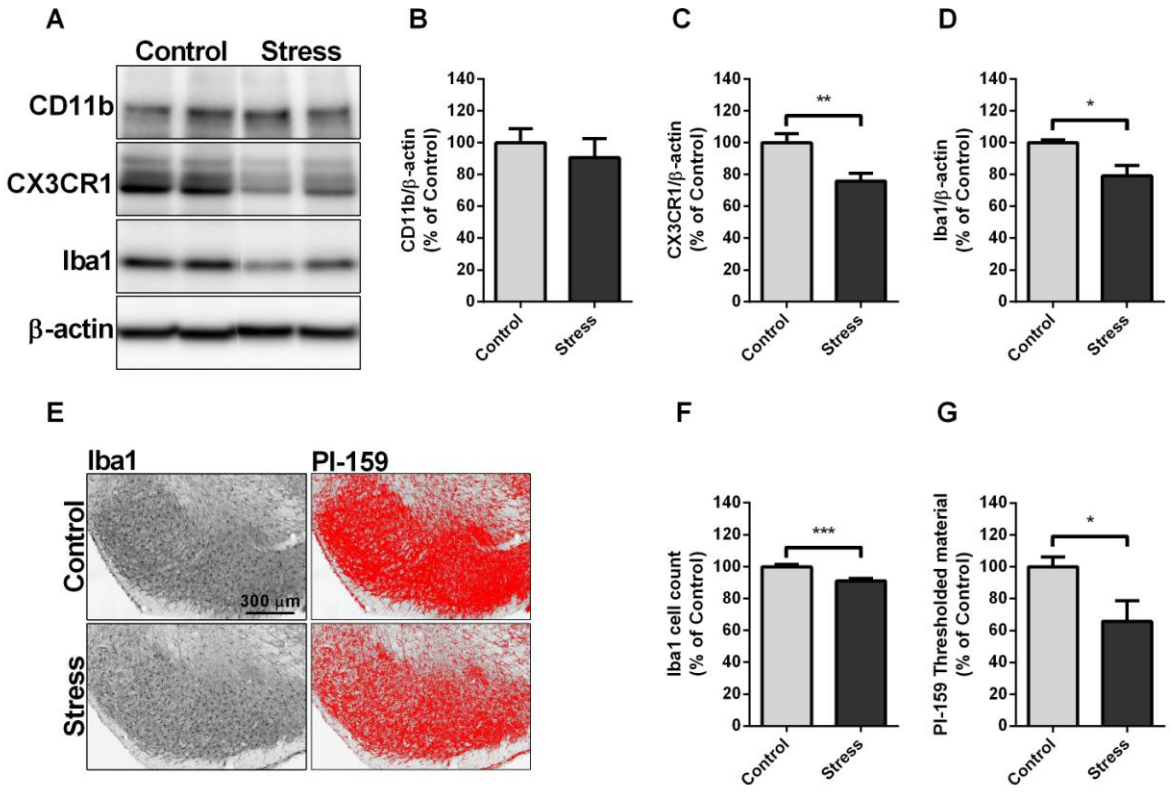

Figure 4.

Microglia markers following chronic restraint stress. A. Representative immunoblots for CD11b, CX3CR1, Iba1 and β-actin from the SN comparing the effects of control and stress. The results for CD11b, CX3CR1 and Iba1 levels were calculated relative to β-actin levels. B. There was no significant change in CD11b levels. Chronic stress significantly reduced C. CX3CR1 and D. Iba1 levels. E. Iba1 staining (left panels) and the material thresholded at pixel intensity (PI) 159 (right panels) of the SN. F. Chronic stress significantly reduced Iba1 positive cells. G. Chronic stress significantly reduced thresholded Iba1 staining at pixel intensity 159.

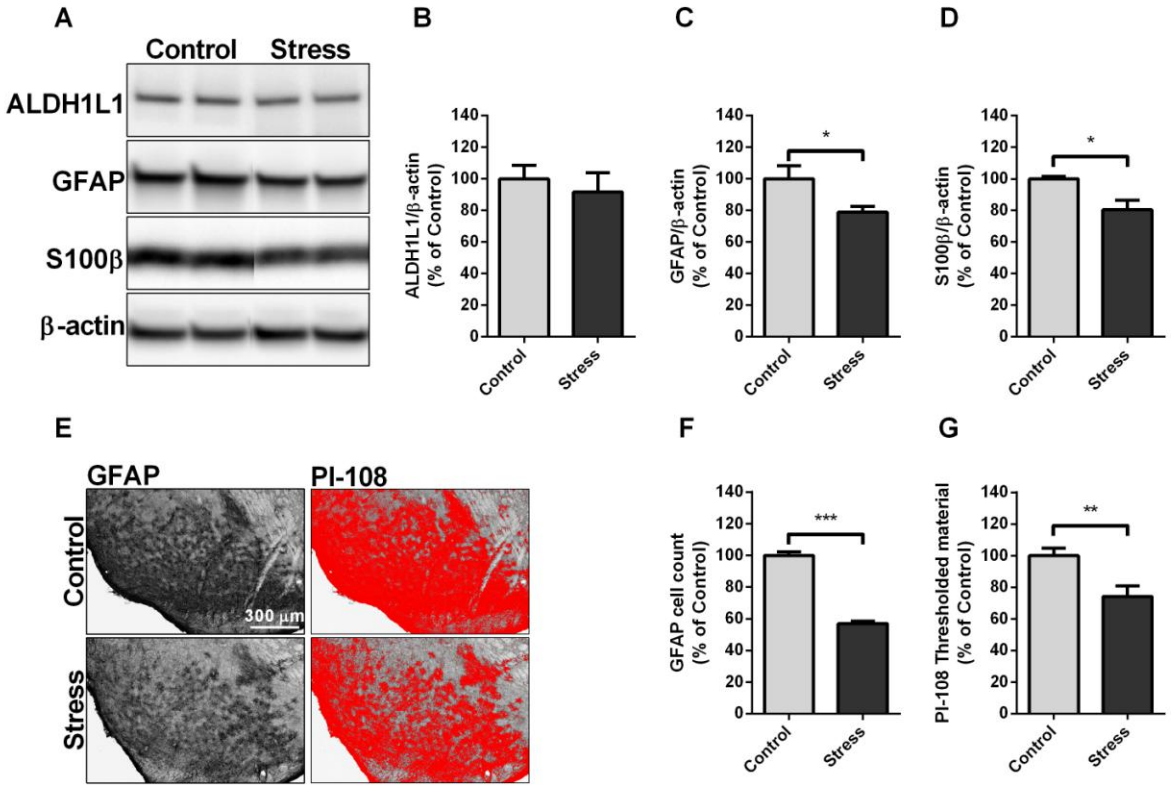

Figure 5.

Astrocytes markers following chronic restraint stress. A. Representative immunoblots for ALDH1L1, GFAP, S100β and β-actin from the SN comparing the effects of control and stress. The results for ALDH1L1, GFAP and S100β levels were calculated relative to β-actin levels. B. There was no significant change in ALDH1L1 levels. Chronic stress significantly reduced C. GFAP and D. S100β levels. E. GFAP staining (left panels) and the material thresholded at pixel intensity (PI) 108 (right panels) of the SN. F. Chronic stress significantly reduced GFAP positive cells. G. Chronic stress significantly reduced thresholded GFAP staining at pixel intensity 108.

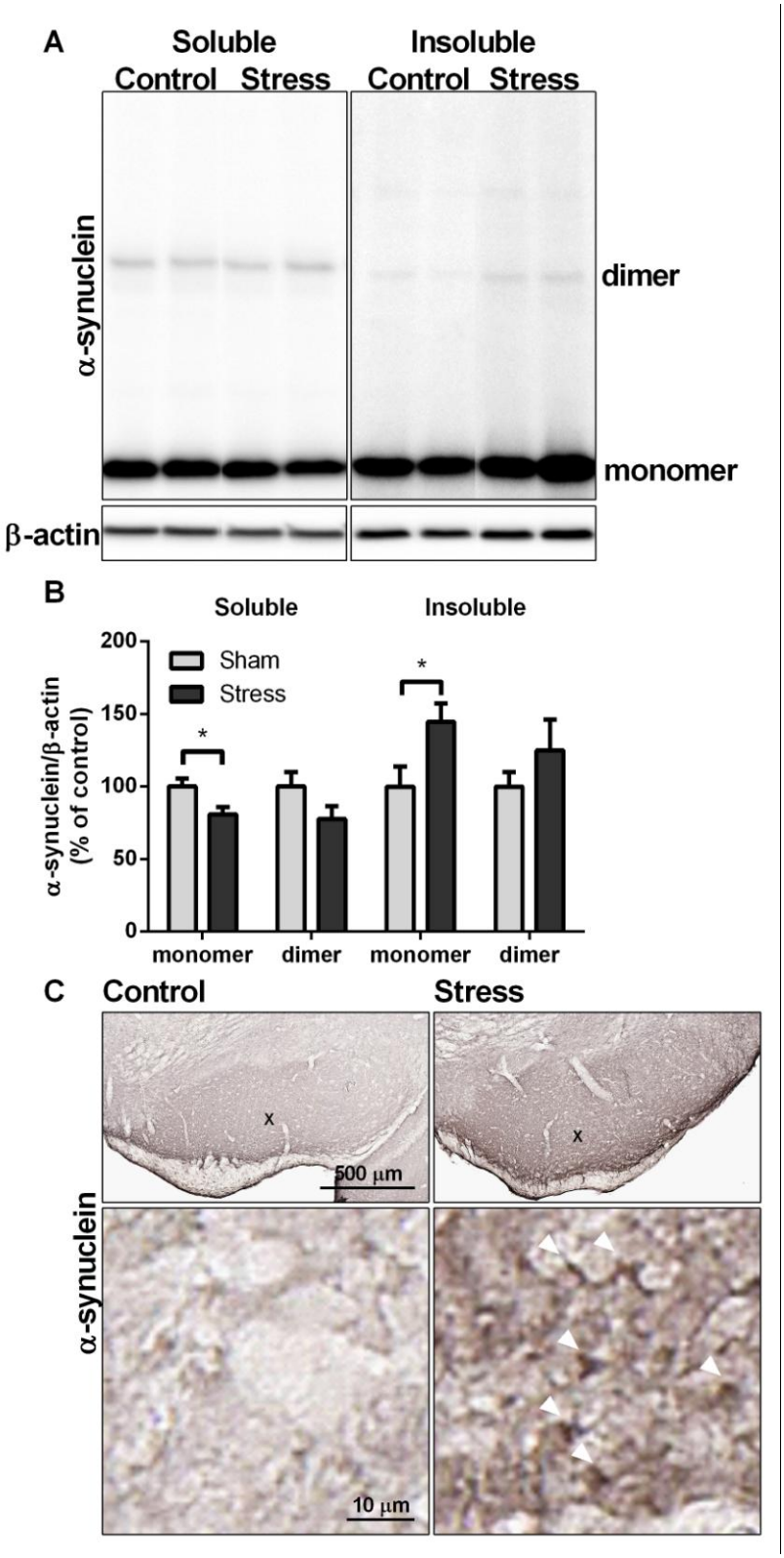

Figure 6.

Aggregation of α-synuclein in the SN following chronic restraint stress. A. Representative immunoblots for α-synuclein and β-actin of the SN soluble and insoluble fractions comparing the effects of control and stress. B. Chronic restraint stress significantly reduced soluble α-

synuclein monomer levels, but significantly increased insoluble α-synuclein monomer levels. C. High magnifying images depicted that chronic stress significantly increased immunostaining of α-synuclein punctae (white arrows) in the SN. Bottom high magnifying (40X) images were directly obtained (marked, X) from top low magnifying (10x) images.

Reconsidering the role of glial cells in chronic stress-induced dopaminergic neurons loss within the substantia nigra? Friend or foe?

Supplementary Material

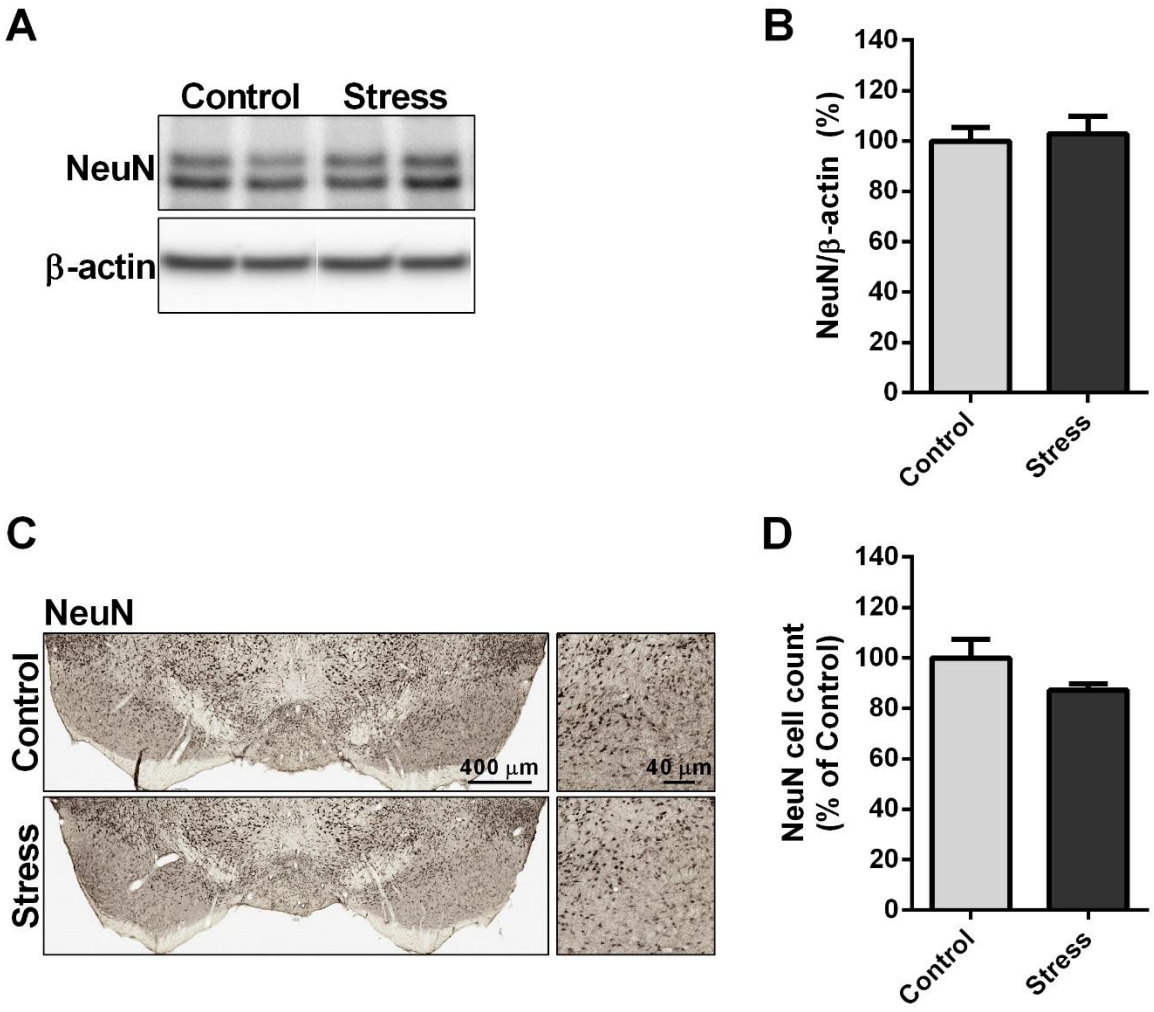

Supplement Figure 1.

Chronic restraint stress induced specific loss of dopaminergic neurons at the SN. A. Representative immunoblots for NeuN and β-actin of the SN comparing the effects of control and stress. C. The results for NeuN protein levels were calculated relative to β-actin levels. There was no significant change in NeuN protein levels. D. NeuN immunostaining in the SN. E. There was no significant change in NeuN positive cells.